

Computational Analysis of Alzheimer's Disease Drug Targets

Shikhar Gupta, Ashish Pandey, Ankit Tyagi and C Gopi Mohan*

Centre for Pharmacoinformatics,
National Institute of Pharmaceutical Education and Research (NIPER),
Sector 67, S.A.S. Nagar- 160 062,
Punjab, INDIA.

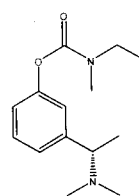
Alzheimer's disease (AD) is a chronic, irreversible and progressive neurodegenerative disorder among aging people. Several cholinesterase inhibitors are nowadays utilized for symptomatic treatment of AD. E2020, marketed as Aricept, belongs to *N*-benzylpiperidine based acetylcholinesterase (AChE) inhibitors and were designed on the basis of computational studies, prior to elucidation of the three-dimensional structure of *Torpedo californica* AChE (TcAChE). E2020 significantly enhances performance in animal models of cholinergic hypofunction. It has a high affinity binding to both electric eel and mouse AChE in the nanomolar range. β -secretase has been shown to be the novel transmembrane aspartic protease, β -amyloid cleaving enzyme 1 (BACE-1). The amyloid hypothesis suggests that the initial cleavage of APP by BACE-1 was a critical step in the process of A β formation, and preventing its production may stop or slow AD progression. These findings prompted extensive structural and functional investigation of BACE-1 as a therapeutic target for the treatment of AD. The present review article focuses on various computational approaches applied in our laboratory to discover and design safer compounds on AD drug targets. An integrated high-throughput *in vitro* screening followed by sequential virtual screening techniques provided us structurally diverse and selective AChE enzyme inhibitors showing promising preliminary pharmacokinetic properties. The combination of these *in silico* methodologies had helped us to virtually screen various chemical libraries to identify new class of compounds that are presumably able to act as dual binding site AChE and BACE-1inhibitors.

Keywords: AChE, ADMET, Screening, Docking, BACE-1, Docking

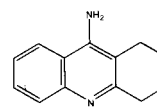
Introduction

Alzheimer's disease (AD) is a chronic, irreversible and progressive neurodegenerative disorder with both genetic and non-genetic causes. According to WHO report AD will grow to nearly 34 million by 2025 and more than 106 million by 2050, and much of this increase will be in the developing countries. Hence there is an urgent need to tackle this life threatening and economically costly disease at the earliest. Two distinct histological changes in the nerve cells of Alzheimer brain are the formation of extracellular amyloid ("senile") plaques and intracellular neurofibrillary tangles, which lead to neurotoxicity. One of the major therapeutic strategies adopted for this disease is primarily symptomatic, based on the cholinergic hypothesis targeting acetylcholinesterase (AChE) enzyme. AChE is a substrate-specific enzyme that degrades the neurotransmitter acetylcholine in the nerve synapses. An optimum level of acetylcholine should be maintained in the brain for its proper function¹.

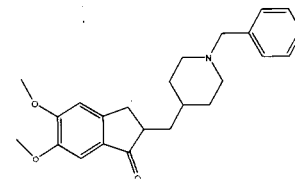
Cholinesterase inhibitors such as rivastigmine, tacrine, donepezil and galantamine, which block the breakdown of acetylcholine, have been used for the treatment of mild to moderate AD²⁻⁴. Recently, memantine, an NMDA receptor antagonist, has been approved for the treatment of moderate to severe AD⁵. All of the above mentioned drugs are reversible inhibitors of AChE, and can restore the level of acetylcholine in the brain of AD patients. The molecular



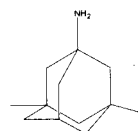
Rivastigmine
(Exelon®)



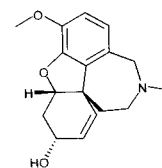
Tacrine (THA,
Cognex®)



Donepezil (Aricept®)



Memantine
(Axura®)



Galanthamine
(Reminyl®)

*Corresponding author

Dr. C. Gopi Mohan

Centre for Pharmacoinformatics,
NIPER S.A.S. Nagar, Punjab-160 062, INDIA.

Phone: 0091-172-2214682-2019

Fax: 0091-172-2214692

E-mail: cmohan@niper.ac.in and

Fig. 1: Some of the well known AChE inhibitors

structures of these drugs are presented in Fig. 1. Considering the mechanism of action of these drugs, they are not expected to interfere with the neurodegenerative cascade of the disease, but only to temporarily mitigate some of the symptoms.

The most common adverse effects of these drugs include nausea and vomiting, both of which are linked to the presence of excess cholinergic neurons. Less common, secondary, adverse effects include bradycardia, muscle cramps, decreased appetite and weight as well as increased gastric acid production⁶⁻⁸.

Experimental evidence suggests that the β -amyloid peptide ($A\beta$) accumulation play a central role in pathophysiology of AD⁹⁻¹⁰. Amyloid plaques, primarily composed of $A\beta$, progressively develop in the brains of AD patients. Mutations in three genes (APP, PS1, and PS2) cause early on-set familial AD by increasing synthesis of the toxic $A\beta_{42}$ peptide. The principal component of amyloid plaque cores is $A\beta$, which is produced during the cleavage of a large transmembrane protein; APP. Mature APP is proteolytically processed by distinct α -secretase and β -secretase pathways. The major route of APP processing is *via* α -secretase, in which APP is cleaved by the protease α -secretase on the C-terminal side generating the large soluble N-terminal APP ($sAPP\alpha$) and a 10kD C-terminal APP fragment that can be further processed by γ -secretase to generate $A\beta_{17-40}$ or $A\beta_{17-42}$, also known as P3 peptides. On the other hand, the β -secretase cleavage yields a truncated soluble APP ($sAPP\beta$) and a membrane bound $A\beta$ containing C-terminal fragment. Further proteolysis of this last fragment by γ -secretase leads to the full length $A\beta_{1-40}$ or $A\beta_{1-42}$ peptide¹¹.

β -Secretase (BACE-1), an aspartyl protease, is an attractive therapeutic target since it plays a key role in the rate-limiting step of $A\beta$ generation¹². In addition, BACE-1 gene knockout homozygote mice showed a complete absence of $A\beta$ production and no obvious deficits in basal neurological and physiological functions¹³. Despite of the success, the actual effects of BACE-1 inhibitors for AD patients need to be further evaluated. It is still important to explore novel drug candidate. Therefore, in response to the molecular complexity of AD, the classic 'one compound, one target' solution may not be effective enough.

Recently interference on $A\beta$ aggregation by AChE inhibitors directed for the development of a novel class of dual binding site inhibitors. Compound binding towards the active gorge site (GS) and peripheral anionic site (PAS) of AChE were defined as dual binding site inhibitors showing both the anti-aggregating $A\beta$ and anti-cholinesterase effect³. Thus compound showing cholinergic activity through AChE inhibition offering a symptomatic relief, with the neuroprotective and disease modifying action of inhibiting the amyloid cascade through β -Secretase (BACE-1) should

alleviate clinical symptoms in short-term therapy, and also prevent the formation of $A\beta$, thereby slowing the progression of the long-term disease.

Various Approaches in the Treatment of Alzheimer's disease

The different pathogenic mechanisms for AD include, loss of cholinergic function (cholinergic replacement therapy and neurotrophins)¹⁴, oxidative stress (antioxidant therapy)¹⁵, the amyloid cascade ($A\beta$) vaccine, γ -secretase inhibitors, statins, inflammatory mediators (NSAIDs), steroid hormone deficiencies (hormone replacement therapy)¹⁶, excitotoxicity (memantine), and the role of dietary factors (low saturated fat diets, moderate alcohol intake)¹⁷.

Role of AChE in Alzheimer's Disease

AD is a multifunctional syndrome with several proteins contributing to its etiology. AChE plays an essential role in cholinergic transmission at both the central and peripheral nervous system. A wide range of evidence showed that AChE inhibitors can interfere with the progression of AD. On the other hand, studies have appeared, suggesting the role of AChE not only in the hydrolysis of the neurotransmitter acetylcholine (ACh), but also in accelerating the aggregation of $A\beta$ into amyloid fibrils¹⁸.

Recently, *in vitro* and *in vivo* studies have consistently demonstrated a link between cholinergic activation and APP metabolism¹⁹. In fact, the long-lasting effects of AChE inhibitors have been recently proposed to be caused by the interference of these drugs with the APP metabolism²⁰. There have been reports on the different putative sites of pharmacological interaction in which the AChE inhibitors are able to interfere with the $A\beta$ metabolism²¹⁻²².

The AChE inhibitors can act through the cholinergic pathway, as elevated levels of ACh would cause muscarinic and nicotinic receptor stimulation. As a result, activation of either or both protein kinase C and mitogen-activated protein kinase pathway would increase $sAPP\alpha$ levels and reduce $A\beta^{23}$ aggregation. Since APP secretion is drastically altered without a concomitant change in intracellular APP levels, this suggests that AChE inhibitors can act at transcriptional or post-transcriptional stages²⁴. After APP protein is synthesized, it proceeds through maturing and sorting with a release of secretory proteins. AChE inhibitors could potentially target any of these steps, which would include glycosylation, phosphorylation and trafficking²⁵.

Moreover, it was also shown that the neurotoxicity of $A\beta_{1-42}$ peptide aggregation depended on the amount of AChE bound to the complexes, suggesting that AChE played a key role in the neurodegeneration observed in AD patient's brain. Thus, inhibition of AChE could influence the APP processing and $A\beta$ deposition, leading to the reduction of one of the pathological expressions of the disease.

Review Article

Thus both cholinergic and amyloid hypotheses are not independent. AChE could play a role during an early step in the development of the senile plaque, as revealed by the finding that the enzyme accelerates A β deposition¹⁸.

Acetylcholinesterase Enzyme

Acetylcholinesterase enzyme (AChE) consists of two types of polypeptide chains, which are each present twice, and have molecular weight of 32KDa. AChE degrades neurotransmitter ACh through its hydrolytic activity to produce choline and an acetate group. The enzyme is mainly found at neuromuscular junctions and cholinergic synapses in the central nervous system, where its activity serves to terminate synaptic transmission. AChE has a very high catalytic activity, and each compound of AChE degrades about 5000 compounds of ACh per second. The choline produced by the action of AChE is recycled - it is transported through reuptake back into nerve terminals, where it is used to synthesize new ACh compounds. AChE is also found on the red blood cell membranes, where it constitutes the Yt blood group antigen. AChE exists in multiple molecular forms, which possess similar catalytic properties, but differ in their oligomeric assembly and mode of attachment to the cell surface.

The crystal structure of *Torpedo californica* AChE (TcAChE) opened up new horizons in research on this enzyme, which had already been the subject of intensive investigation²⁶. As revealed by the crystallographic structure of AChE and its inhibitor complexes, the AChE active site contains a catalytic triad (Ser200, His440, Glu327) located at the bottom of a deep and narrow gorge, lined with aromatic residues and a putative "anionic" subsite located near the bottom of the cavity,²⁷ as shown in Fig. 2.

This subsite binds the quaternary moiety of choline corresponds to a tryptophan residue (Trp84), which stabilises the positive charge of choline by forming a cation- δ complex. Besides the catalytic site, the peripheral anionic site (PAS) of AChE is placed at the mouth of a narrow gorge, about 20 Å deep, at the bottom of which is buried the active site where the hydrolysis of ACh takes place. Recent studies pointed out that the PAS acts as an initial binding site for substrate entry to the acylation site, thus accelerating the hydrolysis of ACh at low substrate concentration.

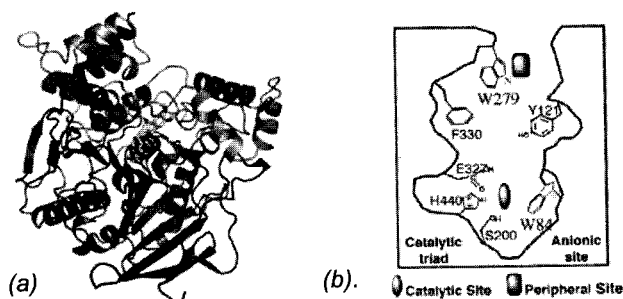


Fig. 2: AChE in complex with donepezil (a) and various binding sites of AChE²⁷ (b).

Beta amyloid cleavage enzyme

β -secretase has long been regarded as therapeutic target for AD in the development of inhibitor drugs for reduction of A β . The cloning and identification of β -secretase, first reported in 1999, invigorated research on both the protease and its inhibitors²⁸⁻³¹. β -secretase as a therapeutic target for AD offers several advantages. First, it initiates the production of A β and is without a compensatory activity, as demonstrated by the lack of A β in β -secretase gene deletion³²⁻³⁴. Inhibition of this target should achieve A β -reduction and thus represents a disease-modifying therapy. It would also eliminate all the harmful downstream steps in the pathogenesis of AD. Further, deletion of the β -secretase gene in mice produced only minor behavioral changes³³⁻³⁴, suggesting that the likelihood of patient safety of a β -secretase inhibitor drug aimed at partial inhibition of the protease activity.

Several proof-of-concept studies have confirmed β -secretase as a therapeutic target for AD. β -secretase inhibitor conjugated to a carrier peptide for penetrating the blood-brain barrier was shown to reach the brain and reduce A β in AD mice³⁵. Immunization of β -secretase that reduced A β in the brain also improved the cognitive performance of AD mice³⁶. Heterozygous β -secretase knock-out transgenic AD mice with 15% reduction of brain A β showed a dramatic reduction of amyloid plaques at old age, suggesting that limited A β reduction may achieve the therapeutic goal³⁷.

Beta amyloid cleavage enzymes- BACE-1 and BACE-2

BACE-1 enzyme cleaves APP at its β -site and between Tyr-10 and Glu-11 of the A β region with comparable efficiency^{38,39}. BACE-2 (also called Asp1) cleaves APP at its β -site and more efficiently at sites within the A β region of APP, after Phe-19 and Phe-20 of A β . These internal A β sites are adjacent to the Flemish APP mutation at residue 21 chromosome, and this mutation markedly increases the proportion of the β -site cleavage product generated by the BACE-2 enzyme. The conservative β -site mutations of APP either increase (the Swedish mutation) or inhibit (M671V) β -secretase activity affecting BACE-1 and BACE-2 activity. The identification of distinct BACE-1 and BACE-2 specificities and a key active-site residue is important for β -site cleavage. This may suggest strategies for selectively inhibiting β -secretase activity of familial AD, and suggest that BACE-2 cleavage of wild-type APP within the A β region can limit production of intact A β in the BACE-2 expressing tissues.

Integration of *in vitro* and *in silico* Study on AChE Inhibitors

We have developed an integrated high-throughput *in vitro* screening followed by molecular docking and ADMET studies, which provided structurally diverse and selective AChE enzyme inhibitors. High throughput *in vitro* screening

(bioassay) was performed on a structurally diverse set of compounds towards AChE inhibition. The data was obtained using a well-recognized and robust assay based on Ellman's reaction that was optimized to be conducted in 384-well plates in an automated environment⁴⁰. The three most active hits were identified (compounds 1, 2, 3), which displayed $IC_{50(AChE)}$ values of 0.063; 0.019 and 0.069 μM , respectively, within the same range of IC_{50} value obtained for the known AChE inhibitor, physostigmine (0.04 μM) at the used substrate concentration of 2.7 μM ⁴¹. The structure of the compounds are shown in Fig. 3.

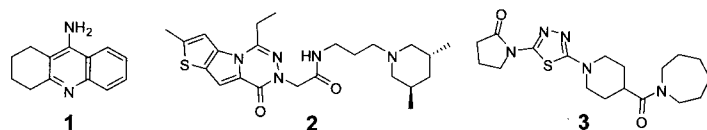


Fig. 3: Structure of three most active compounds identified by in-vitro screening.

Two of these compounds were new (compounds 2 and 3) and the third turned out to be the known AChE inhibitor, tacrine (compound 1), which unexpectedly served as a reference compound. The effect at different concentrations was also studied in the assay format in which the reaction was started by adding the enzyme. Potency of the three best hits was similar, and thus confirmed to be independent of the assay variant. These compounds could be further explored for clinical studies for the treatment of AD.

Docking study was performed on these two structurally diverse and dual binding site AChE inhibitors using the FlexX module in the SYBYL7.1 software, and binding mode analysis using the ligand-receptor interaction module of MOE software (Chemical Computing Group Inc, US). Docking analysis was performed at the gorge site and PAS. Donepezil, an FDA approved drug was used as a reference dual binding site inhibitor for docking analysis, using the *Torpedo californica* AChE crystal structure (PDB code: 1EVE), considering that the size and shape complementarity of donepezil is similar to the most potent inhibitor 2 of the data set (Table 2). FlexX analysis showed that the most potent inhibitor, 2 ($IC_{50} = 0.019 \mu M$), docked

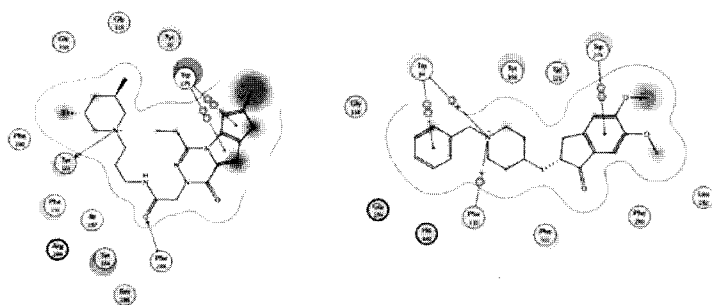


Fig. 4: Docking analysis of the most potent compound 2 from the present data set (a) and Donepezil (b), at the AChE enzyme active site (PDB code 1EVE).

well at the AChE catalytic pocket with a high docking score -17.3. The docking of donepezil, ($IC_{50} = 0.023 \mu M$), to the same crystal structure (PDB code: 1EVE) produced a docking score of -13.8. We obtained a similar binding mode at the bottom, middle and entrance of the AChE gorge site, when compared with that of the crystal structure of AChE in complex with donepezil. The lesser docking score of donepezil w.r.t that of the most potent compound 2 could be attributed for its low activity. For simplicity, we have presented only the results obtained for these two docked compounds (Figs. 4a & 4b).

ADMET Analysis

Absorption, distribution, metabolism, excretion and toxicity (ADMET) profile of FDA approved AD drugs, well known AChE inhibitors and our 2 most potent all compounds were performed using the Cerius2 software package. A comparative ADMET analysis, of the FDA approved drugs, lead compounds and three most potent compounds from the present data set, is presented in Table 1. The most potent compound 2 of the AChE dataset was comparable with the ADMET properties observed by FDA approved drugs. This led us to conclude that compound 2, the most potent compound, was safe from ADME properties and organ toxicity.

Table 1 : ADMET prediction on FDA approved drugs, lead compounds and most potent compounds from the data set using Cerius2 software.

Molecular Property	MW	Rot. Bond	HBA	HBD	AlogP	LogD	AAb	ABBBL	ASL	AH	ACyp.
Acceptable Range	<500	<10	<10	<5	<5	<5	<10	4 to 2	0 to 4	0	0
FDA approved drug compounds											
Tacrine	198.2	0	1	2	2.28	3.053	0	1	2	1	0
Galanthamine	287.3	2	4	1	1.39	1.440	0	2	3	0	1
Donepezil	379.5	6	4	0	3.69	3.245	0	1	2	0	1
Rivastigmine	250.3	6	3	0	2.41	1.605	0	1	3	0	1
Lead compounds											
Decamethonium	258.5	11	0	0	2.07	1.198	1	4	4	0	0
(-)-Huprine Y	298.8	1	2	2	3.64	4.768	0	1	1	0	1
Propidium	417.6	7	1	4	2.30	1.405	0	2	3	0	1
AP2238	415.5	7	5	0	4.47	4.597	0	1	2	1	1
Most potent compounds from the data set											
1	198.2	0	1	2	2.28	3.053	0	1	2	1	0
2	443.6	7	5	1	2.59	1.896	0	2	2	0	0
3	377.5	3	5	0	1.99	1.228	0	2	3	1	0

MW = Molecular Weight; Rot. Bond = Rotatable Bond; HBA = Hydrogen bond acceptor; HBD = Hydrogen bond donor; AlogP = Atomic logP value; LogD = lipophilicity value; AAb = ADME_Absorption_Level_2D; ABBBL = ADME_BBB_Level_2D; ASL = ADME_Solubility_Level; AH = ADMET_HEPATOX; ACyp = ADMET_CYP2D6.

In vitro and Computational study of Coumarin 106 interaction with AChE

The first study with the coumarin library was performed using a 96-microtiter well plate assay based on Ellman's reaction. Coumarins were assayed at 5 and 30 μM , and coumarin 106 was found the most active inhibitor at both concentrations. The follow-up analysis using kinetic studies demonstrated that coumarin 106 displays mixed-type AChE

inhibition with a $pIC_{50} = 4.97 \pm 0.09$ and $K_i = 2.36 \pm 0.17 \mu M$. The ability of this molecule to interact with AChE was further confirmed through computational studies, in which a primary binding was proved to occur at the active gorge site, while a secondary binding was demonstrated at the peripheral anionic site. Also, coumarin 106 was shown to inhibit butyrylcholinesterase (BChE) with slightly lower potency ($pIC_{50} = 4.56 \pm 0.06 \mu M$), and found to be non-toxic in Caco-2 cells. The combination of these findings makes coumarin 106 an attractive molecule for further investigation. This is the first report where AChE inhibitory activity has been associated with coumarin 106, and proof has been given of its convenience as a lead molecule.

A binding study of coumarin 106 was performed using ligand-receptor interaction module of MOE software (Chemical Computing Group Inc., USA), while docking analysis was conducted using FlexX software (Sybyl 7.1). In this study, galanthamine was used as a reference inhibitor in *Torpedo californica* AChE crystal structure (PDB code: 1QTI), considering that size and shape complementarity of galanthamine is similar to coumarin 106⁴².

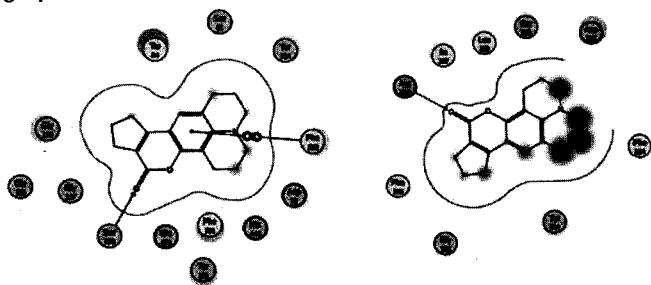


Fig. 5 : Docking analysis of the Coumarin 106 at the enzyme active site (a) and Coumarin 106 at the peripheral anionic site of enzyme (b).

The compound docked at the active gorge site, using FlexX software for which the total score obtained was 10.9, as shown in Fig. 5a. A hydrogen bonding interaction between the carbonyl group of coumarin 106 and the hydroxyl group of Ser200, together with π - π stacking interaction between coumarin 106 with Phe330 are proposed to occur during the primary binding to the active site⁴³. Also, a secondary interaction is prone to take place with the PAS of AChE, as presented in Fig. 5b. In this case, the total score obtained was 10.1, and the interaction seems to occur between the carbonyl group of coumarin 106 and the amide group of Arg289.

Structure-Based Design of BACE-1 Inhibitors

Several crystal and co-crystal structures are available for the BACE-1 enzyme⁴⁴⁻⁴⁶. Using the knowledge of the active site of BACE-1 crystal structure (Fig. 6) various new compounds have been designed recently.

Detail knowledge of the active site and catalytic process had a strong influence on the strategy of β -secretase inhibitor development. Alignment of crystal structure of



Fig. 6 : BACE-1 (PDB Code : 2HM1) crystal structure co-crystallized with inhibitor, generated using the program PYMOL.

BACE-1(PDB code 1W51), and BACE-2 (PDB code 2EWY) sequences suggested that Arg296 of BACE-1 (Arg310 of BACE-2) could form a salt bridge with the Asp immediately after the β -site of APP (APP residue 672, A β residue 1). Some scientist speculated that the internal A β proteolysis by BACE-2 would be less sensitive to perturbations of this Arg because these sites did not include an immediately adjacent acidic amino acid. These data are consistent with the formation of a salt bridge between Asp672 of APP (A β residue 1) and Arg296 and Arg310 of BACE-1 and BACE-2, respectively.

BACE-1 belongs to the aspartyl protease class of catabolic enzymes. The main strategies toward aspartyl protease inhibitor design rely on active engagement of the catalytic dyad for their intrinsic potency. Recently there have been reports of inhibitors that do not directly engage the catalytic aspartates but interact through a water mediated hydrogen bond which displays modest inhibition of BACE-1 ($IC_{50} = 24 \text{ nM}$) with no interaction with the catalytic dyad or primary active site region. A small compound inhibitor of BACE-1 with a unique binding mode has been developed. This novel binding mode for BACE-1 may offer alternative approaches to the current drug design effort in aspartyl proteases.

Design of Selective BACE-1 and BACE-2 Inhibitors

QSAR is one of the most important areas in chemoinformatics and its advances have widened the scope of rational drug design and the search for the mechanism of drug action. It is a well-established fact that the chemical and pharmacological effects of a compound are closely related to its physico-chemical properties, which can be calculated by various methods from the molecular structure. Recently, we have proposed pharmacophore model derived from the 3D-QSAR study on forty-three hydroxyethylamine derivatives. This model gives an idea about the important features to design selective BACE-1 enzyme inhibitor⁴⁷.

Three-dimensional QSAR (3D-QSAR) can be derived by sampling the steric and electrostatic fields surrounding a

set of ligands and correlating the difference in these fields to the biological activity. CoMFA and CoMSIA calculate at each lattice points the steric (S) field using Lennard-Jones potential and the electrostatic (E) field using Coulomb potential. In addition to this CoMSIA also calculates the hydrophobic (H) field, the hydrogen bond acceptor (A) field, and the hydrogen bond donor (D) field at each lattice point.

3D-QSAR models were developed based on comparative molecular field analysis (CoMFA) and comparative molecular similarity indices analysis (CoMSIA), on a series of 43 hydroxyethylamine derivatives with their IC_{50} values ranging from 1 to 7,950 nM, acting as potent inhibitors of α -site amyloid precursor protein (APP) cleavage enzyme (BACE-1). The crystal structure of the BACE-1 enzyme (PDB ID: 2HM1) with one of the most active compound was available, and we assumed it to be the bioactive conformation of the studied series, for 3D-QSAR analysis. The whole data set was divided into a training set of 34 compounds to generate the QSAR models and a test set of 9 compounds to evaluate the predictive ability of the developed models.

The most active compound was extracted from the crystal structure, and subjected to constrained geometry optimization using the Powell method by applying Gasteiger-Hückel charges. The geometry of the compound was optimized only to the added hydrogen, and not to the basic scaffold, to preserve its experimental model structure, the so-called bioactive conformation. The rest of the 42 compounds were built by modifying the required substitution on this bioactive conformation of the most active compound.

The most important requirement for 3D-QSAR (CoMFA and CoMSIA) analysis is that the structures to be analyzed be aligned according to a suitable 3D conformational template, which is assumed to be a bioactive conformation. In the present study, co-crystal structure-guided bioactive conformation of the template of most active compound was used for alignment of the other 42 compounds in the series, by the common substructure alignment, using the ALIGN DATABASE command in SYBYL software. In this alignment procedure each compound was aligned to the template by rotation and translation, so as to minimize the root-mean-square deviation between the atoms in the template and the corresponding atoms in the analog.

The statistical results of the CoMFA and CoMSIA PLS analysis are presented in Table 3. The constructed CoMFA model is robust, and the ratio of steric (S) to electrostatic (E) fields was found to be 47.4:52.6, which implies that the electrostatic part makes a larger contribution to interaction with the BACE-1 enzyme. The constructed CoMSIA model is robust and the percentage different field contributions include: steric (S)- 24.8, electrostatic (E)- 34.0, hydrophobic (H)- 26.3 and hydrogen bond donor (HD)- 14.9. This implies that the E part makes a larger contribution, followed by H, S, and HD, for interaction of inhibitor with the BACE-1 enzyme. Scatter plots for actual

Table 3: PLS summary of CoMFA and CoMSIA results

Statistical Parameters	CoMFA (S E)	CoMSIA (S E H D)
Number of compounds in training set	34	34
Number of compounds in test set	9	9
r^2_{cv}	0.810	0.754
NOC	7	4
SEE	0.063	0.204
R^2	0.998	0.978
F-test	209.08	324.673
r^2_{bs}	0.999	0.989
SD_{bs}	0.001	0.006
r^2_{pred}	0.934	0.750
Percentage of field contributions		
S	47.4	24.8
E	52.6	34.0
H	—	26.3
D	—	14.9

Abbreviations: S (Steric field), E (Electrostatic field), H (Hydrophobic field), D (Hydrogen bond donor field)

r^2_{cv} = Cross-validated correlation coefficient by PLS LOO method

NOC = Optimum number of components as determined by PLS LOO cross validation study

SEE = Standard error of estimate

r^2 = Conventional correlation coefficient

r^2_{bs} = Correlation coefficient after 100 runs of bootstrapping

SD_{bs} = Standard deviation from 100 runs of bootstrapping

r^2_{pred} = Predictive correlation coefficient

(experimental BACE-1) versus predicted activities of training-set (blue points) and test-set (magenta points) compounds, obtained using the CoMFA and CoMSIA analysis, are shown in Figs. 8a and 8b, respectively.

CoMFA and CoMSIA model is usually represented as 3D coefficient contour maps which surround all the lattice point, where the QSAR is found to contribute with the change in the interaction energy or the binding affinity with respect to its structural changes.

In the CoMFA and CoMSIA analysis it was noted that the percentage contribution of the electrostatic (E) field was prominent, i.e., 52.6 and 34.0. This clearly predicts that the E chemical feature dominates in comparison with other fields such as S, H, and D for potent BACE-1 enzyme inhibitory action. Appearance of the different blue contour

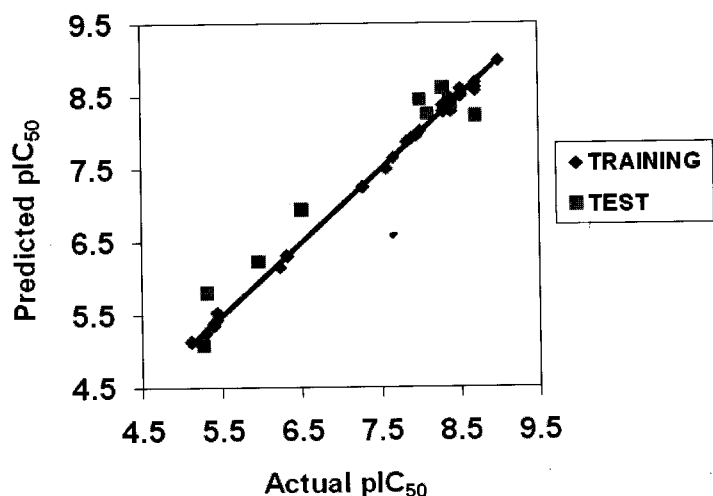


Fig. 8a : Correlation plot of actual (experimental) activities and CoMFA predicted activities of the training set (blue points) and test set (magenta points) compounds obtained using CoMFA analysis.

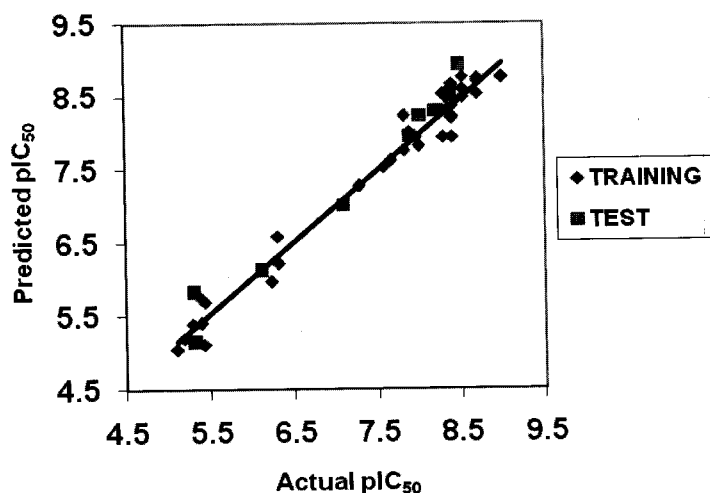


Fig. 8b : Correlation plot of actual (experimental) activities and CoMSIA predicted activities of the training set (blue points) and test set (magenta points) compounds obtained using CoMSIA analysis.

regions shown in Figs. 9(a, b) corresponds to the different active site regions of the BACE-1 enzyme together with an active compound.

Figures 9 (a, b) depicts the CoMFA and CoMSIA electrostatic contour maps together with the compound **23**. Positive-charge-favored blue contours were found near the S-1 sub-site, which correspond to the difluoro phenyl group of compound **23**. This group is commonly present in majority of the studied compounds. Figures 9(c,d) depict the CoMFA and CoMSIA steric contour maps together with compound **23**. Sterically favorable and unfavorable regions in both these contour maps showed some contradictions. CoMFA contour map together with compound **23** showed sterically favored green contours near some of the selective regions of the S-2 and S-3 subsites, whereas sterically

unfavoured yellow contours are also seen near these subsites as shown in Fig. 9c. CoMSIA contour map together with compound **23** showed sterically favored green contours near some of the selective regions of the S-2 and S-3 subsites, whereas sterically unfavoured yellow contours are also seen near these subsites as presented in Fig. 9c. CoMSIA contour map together with compound **23** showed sterically favorable (green contours) regions near the S-1, S-2, S-2', and S-3 subsites, as presented in Fig. 9d. Small yellow contours do appear near these subsites, showing different sterically unfavorable regions.

These analyses clearly reflect that substitution of optimum bulky groups at these regions might enhance the compound's BACE-1 inhibitory activity. CoMSIA hydrophobic contour map together with compound **23** presented in Fig. 9e shows white contours (favorable for hydrophilic groups) near the S-2 and S-3 pockets and yellow contours (favorable for hydrophobic groups) near the S-1, S-2, and S-2' pockets. CoMSIA hydrogen bond donor contour map together with compound **23**, presented in Fig. 9f, shows purple contours (favorable for acceptor atom substitutions) near the S-1, S-2, and S-3 pockets and cyan contours (favorable for donor atom substitutions) near the S-1 pocket. These maps clearly predict the nature of the chemical environment required for better binding of compound with the BACE-1 enzyme.

Design of selective and specific BACE-1 inhibitors is rather challenging due to the close homology with other A1 aspartic family members, such as BACE-2, pepsin A and C, renin, and cathepsin D and E⁴⁸. The following points should be noted from the BACE-1 (or BACE-2) crystal structure analysis.

(i) The pockets that are formed by the C-terminal domain, namely S-2, S-1', and its neighboring regions, are more solvent-exposed and hydrophilic in the BACE-1 and BACE-2 enzymes as compared with the other aspartic proteases. These regions are central to the design of BACE-specific inhibitors [residues Arg235 (Arg248) of S-2 and Lys224 (Lys227) of S-1' in BACE-1(BACE-2) respectively]. CoMFA electrostatic contour map together with compound **23**, depicted in Fig. 9a, shows blue contours near S-2 (also small red contours) and S-1', favoring electropositive groups at this region. However, the CoMSIA electrostatic contour map together with compound **23**, presented in Fig. 9b, shows red contours near the S-2 pocket, and no electrostatic component appeared near the S-1' pocket, thus partially supporting its corresponding CoMFA contour map (Fig. 9a).

(ii) The S-3 subpocket of the BACE and renin enzymes have alanine (Ala335 of BACE-1) residue, while in pepsin A and C as well as cathepsin D and E have an acidic environment due to aspartic acid side-chain present in this region. The sequence-structural differences in these families of enzymes might be crucial for its unfavorable physicochemical environment, i.e., electrostatic, steric, and other enzyme-inhibitor interactions⁴⁸. Thus compounds occupying the S-3 subpocket and designed for BACE

inhibitors might not be acceptable for other A1 aspartic proteases. The present CoMSIA analysis has also shown green/yellow contours near the S-3 pocket (Fig. 8, 9c, d) suggesting mixed-type behavior (sterically optimal region) in support of the crystal structure analysis, explained above.

(iii) Close homology of the BACE-1 and BACE-2 enzyme increases the complexity of designing more selective BACE-1 or BACE-2 inhibitors. Crystal structure analysis has further revealed some key differences between these enzymes, i.e., near the nonprime binding site (S-3 pocket), Ile110 and Ser113 of BACE-1 was replaced with Leu126 and Ile129 in BACE-2 enzyme. This should direct towards fine-tuning of inhibitor size, shape, etc. in order to create better physicochemical environment for selective interactions with the enzyme⁴⁸. As mentioned above, the CoMSIA interaction energy map also supported this result and suggests substitution/modification of sterically optimal groups near the nonprime binding site (Figs. 9c, d). CoMSIA hydrophobic contour map together with compound **23**, does not show any hydrophobically favored /unfavoured regions (Fig. 9e); CoMSIA hydrogen bond donor map together with compound **23** shows purple contours near the S-3 pocket (Fig. 9f), suggesting that acceptor atom substitution at this part of the compound might help in the design of selective and more potent BACE-1 inhibitors. (iv) Loop region, i.e., the S-2 pocket, Gln12 and Asn233 of BACE-1 (Arg28 and

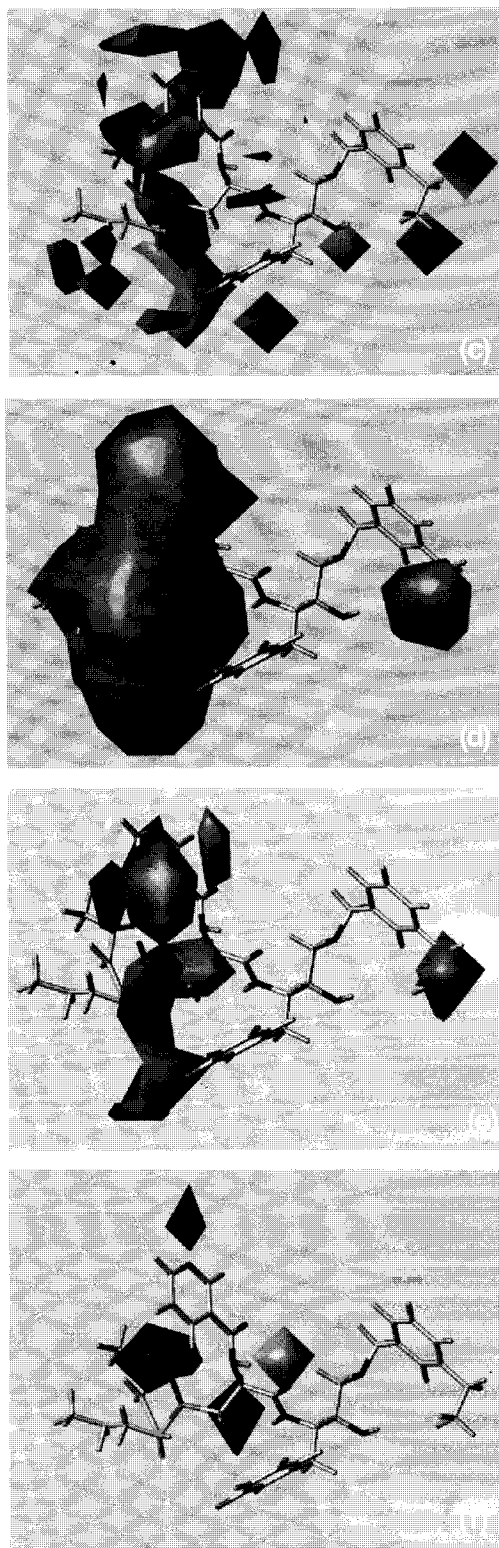


Fig. 9: (a) CoMFA STDEV*COEFF electrostatic contour map together with compound **23**, (b) CoMSIA STDEV*COEFF electrostatic contour map together with compound **23**, (c) CoMFA STDEV*COEFF steric contour map together with compound **23**, (d) CoMSIA STDEV*COEFF steric contour map together with compound **23**, (e) CoMSIA STDEV*COEFF hydrophobic contour map together with compound **23** and (f) CoMSIA STDEV*COEFF hydrogen bond donor contour map together with compound **23**.

Leu246 of BACE-2), was also important to distinguish between these enzymes.

(v) The prime binding site was also crucial for selective binding of the inhibitors with the BACE-1 (or BACE-2) enzyme. The key differences in the prime binding site residues are: Ile126, Arg128, and Thr329 of BACE-1 were replaced with Leu142, Lys144, and Asn341 of the BACE-2 enzyme. The CoMFA and CoMSIA interaction energy maps (Figs. 9a-f) and the pharmacophore model (Fig. 10) derived from this analysis broadly supported these five points. Furthermore, the integration of the crystal structure information with the 3D-QSAR analysis might be promising for the design of more potent and selective BACE-1 inhibitors.

Conclusions

Multiple etiologies are thought to contribute to the neurodegenerative process of the AD. Molecules that modulate the activity of a single protein target are unable to significantly modify the progression of the disease. It is well established that AChE and BACE-1 are the key enzymes that involved in initiation and aggregation of A β . Considering these facts we have developed a strategy to identify novel dual inhibitors of AChE and BACE-1 enzyme. Multi-target directed drugs have been to be found effective in controlling complex CNS diseases. Here we have performed the docking study on dual binding site of AChE inhibitors and comparative ADMET analysis with the existing drugs and lead molecules.

Three-dimensional QSAR models for 43 hydroxyethylamine derivatives of BACE-1 inhibitors were developed using CoMFA and CoMSIA techniques. The selectivity of the BACE-1 inhibitors with respect to other aspartic proteases also emerged from this study. Thus, information gathered from the 3D-QSAR contribution maps, and the developed pharmacophore model shed some light on the effects of the substitution pattern related to the biological activity within this series of anti-Alzheimer compounds. This analysis could broadly support the rational design of potential drug candidates with improved BACE-1 inhibitory activity.

References :

1. Stahl SM, *The Journal of Clinical Psychiatry*. 2000, 61, 813-814.
2. Silmana I, Sussman JL, *Chemico-Biological Interactions*. 2008, 175, 3-10.
3. Raschetti R, Albanese E, et al., *PLoS Medicine*. 2007, 4, 1818-1828.
4. Raina P, Santaguida P, Ismaila A, et al., *Annals of Internal Medicine*. 2008, 148, 379-397.
5. A. Areosa Sastre, F. Sherriff, et al., *Cochrane Database of Systematic Reviews*. 2004, 4, CD003154
6. Mayeux R, Sano M, *The New England Journal of Medicine*. 1999, 341, 1670-1679.
7. Selkoe DJ, *Nature*. 1999, 399, A23-A31.
8. Yankner BA, *Neuron*. 1996, 16, 921-932.
9. Cole SL and Vassar R, *Current Alzheimer Research*. 2008, 5, 100-120.
10. Guo T and Hobbs DW, *Current Medicinal Chemistry*. 2006, 13, 1811-1829.
11. Dingwall C, *Journal of Clinical Investigation*. 2001, 108, 9, 1243-1246.
12. Sinha S, Lieberburg I, *Proceedings of National Academy of Science*. 1999, 96, 11049.
13. Luo Y, Bolon B, et al., *Nature Neuroscience*. 2001, 4, 231.
14. John B and Standridge MD, *Clinical Therapeutics*. 2004, 26.
15. Mary Sano and Christopher E, *The New England Journal of Medicine*. 1997, 336, 1216-22.
16. Dominguez DI and Strooper BD, *Trends in Pharmacological Sciences*. 2002, 23.
17. Barry Reisberg MD and Rachele DM, et al., *Journal of Medicinal Chemistry*. 2003, 348, 1333-41.
18. Inestrosa NC, Alvarez A, et al., *Current Alzheimer Research*. 2005, 2, 301-306.
19. Verhoeff NP, *Expert Review of Neurotherapeutics*. 2005, 5, 277-84.
20. Liu HC, Chi CW, et al., *Dementia and Geriatric Cognitive Disorders*. 2005, 19, 345-48.
21. Racchi M, Mazzucchelli M, et al., *Chemico-Biological Interactions*. 2005, 157-158, 335-38.
22. Zhang X, *Current Drug Targets - CNS & Neurological Disorders*. 2004, 3, 137-152.
23. Nitsch RM, Slack BE, et al., *Science* 1992, 258, 304-307.
24. Lahiri DK, Nall C, *Molecular Brain Research*. 1995, 32, 233-240.
25. Buxbaum JD, Greengard P, *Annals of the New York Academy of Sciences*. 1996, 777, 327-31.
26. Sussman JL, Harel M, et al., *Science*. 1991, 253, 872-879.
27. Kryger G, Silman I, Sussman JL, *Structure*. 1999, 7, 297-307.
28. Vassar R and Bennett BD, *Science*. 1999, 286, 735-741.
29. Lin X and Koelsch G, *Proceedings of the National Academy of Sciences*. 2000, 97, 1456-1460.
30. Sinha S and Anderson JP, *Nature*. 1999, 402, 537-540.
31. Hussain I and Powell D, *Molecular and Cellular Neuroscience*. 1999, 14, 419-427.
32. Cai H, Wang Y and McCarthy D, *Nature Neuroscience*. 2001, 4, 233-234.
33. Luo Y, Bolon B and Kahn S, *Nature Neuroscience*. 2001, 4, 231-232.
34. Roberds SL and Anderson J, *Human Molecular Genetics*. 2001, 10, 1317-1324.
35. Chang WP and Koelsch G, *Journal of Neurochemistry*. 2004, 89, 1409-1416.
36. Chang WP and Downs D, *Federation of American Societies for Experimental Biology*. 2007, 21, 3184-3196.
37. McConlogue L and Buttini M, *Journal of Biological Chemistry*. 2007, 282, 26326-26334.
38. Hussain I and Powell D, *Molecular and Cellular Neuroscience*. 1999, 14, 6, 419-427.
39. Bennett BD and Denis P, *Journal of Biological Chemistry*. 2000, 275, 37712-37717.
40. Ellman GL, Courtney KD, et al, *Biochemical Pharmacology*. 1961, 7, 88-95.
41. Jarvinen P, Fallarero A, Gupta S, Mohan CG, et al., *Combinatorial Chemistry and High Throughput Screening*. 2010, 13, 3, 278-284.
42. Fallarero A, Oinonen P, Gupta S, Blom P, Galkin A, Mohan CG, et al., *Pharmacological Research*. 2008, 58, 3-4, 215-221.
43. Freskos J N and Fobian Y M, et al., *Bioorganic & Medicinal Chemistry Letters*. 2007, 17, 1, 73-77.
44. Beswick P and Charrier N, et al., *Bioorganic & Medicinal Chemistry Letters*. 2008, 18, 1022-1026.
45. Park H and Min K, et al., *Bioorganic & Medicinal Chemistry Letters*. 2008, 18, 2900-2904.
46. Iserloh U Y, et al., *Bioorganic & Medicinal Chemistry Letters*. 2008, 18, 1, 414-417.
47. Ashish P, Jignesh M and Mohan CG, *Molecular Diversity*. 2009, 14, 1, 39-49.
48. Ostermann N, Eder J, Eidhoff U, et al., *Journal of Molecular Biology*. 2006, 355, 249-261.